J. Fluid Mech. (1995), *vol.* 287, *pp.* 225–249

Finite-amplitude convection in the presence of an unsteady shear flow

By PHILIP HALL

Department of Mathematics, University of Manchester, Manchester M13 9PL, UK

(Received 25 October 1993 and in revised form 21 October 1994)

The effect of an unsteady shear flow on the planform of convection in a Boussinesq fluid heated from below is investigated. In the absence of the shear flow it is well-known, if non-Boussinesq effects can be neglected, that convection begins in the form of a supercritical bifurcation to rolls. Subcritical convection in the form of say hexagons can be induced by non-Boussinesq behaviour which destroys the symmetry of the basic state. Here it is found that the symmetry breaking effects associated with an unsteady shear flow are not sufficient to cause subcritical convection so the problem reduces to the determination of how the orientations of roll cells are modified by an unsteady shear flow. Recently Kelly & Hu (1993) showed that such a flow has a significant stabilizing effect on the linear stability problem and that, for a wide range of Prandtl numbers, the effect is most pronounced in the low-frequency limit. In the present calculation it is shown that the stabilizing effects found by Kelly & Hu (1993) do survive for most frequencies when nonlinear effects and imperfections are taken into account. However a critical size of the frequency is identified below which the Kelly & Hu (1993) conclusions no longer carry through into the nonlinear regime. For frequencies of size comparable with this critical size it is shown that the convection pattern changes in time. The cell pattern is found to be extremely complicated and straight rolls exist only for part of a period.

1. Introduction

Our concern is with the effect of an unsteady shear flow on the evolution of convection rolls in a Boussinesq fluid. In recent papers, Kelly & Hu (1993,1994) showed that a time-periodic, non-planar shear flow can significantly stabilize a fluid layer heated from below. Subsequently Hall & Kelly (1994) showed that steady and unsteady shear flows remove the preference for hexagonal shaped cells at the onset of convection in a non-Boussinesq fluid. Essentially this is achieved by splitting sufficiently far apart the critical Rayleigh numbers for the triad of roll disturbances which combine to form a hexagonal cell.

The stabilizing mechanism found by Kelly & Hu (1993) can perhaps be explained by the well-known results for convection in a steady unidirectional flow; see for example the recent review by Kelly (1994). If a layer of fluid heated from below is subject to shear flow in the x-direction then it is easy to show that the critical Rayleigh number for rolls aligned with the x-axis is not altered by the flow. However, rolls aligned at any non-zero angle to the x-axis are stabilized by the shear, and, at small flow Reynolds numbers R_e, the increase in the critical Rayleigh number is of order R_e^2. For non-planar shear flows general disturbances cannot align themselves with the shear

and stabilization results. Kelly & Hu (1993) found that an oscillatory non-planar shear flow has a maximum stabilizing effect at low frequencies (for sufficiently high values of the Prandtl number). This is exactly what we would expect if the stabilizing effect of a unidirectional flow were, in some sense, integrated over time and all roll orientations.

In the present paper we will focus on the nonlinear selection process for convection in the presence of a low-frequency shear flow induced by oscillations of the lower wall. We choose to concentrate on the low-frequency regime because it is here that the stabilizing effect found by Kelly & Hu (1993) is generally most pronounced and because Kelly & Hu's linear analysis needs clarification there. Thus we shall look at the interaction of all possible roll disturbances at a given Rayleigh number. We note that hexagonal cells are not possible for a Boussinesq fluid in the presence of a small-amplitude unsteady shear flow. This is in contrast to the case investigated by Roppo, Davis & Rosenblat (1984) who found that a periodic modulation of the boundary temperature conditions could induce hexagonal convection. Here the situation is different because the leading-order temperature gradient is still linear, and the analysis of Hall & Kelly (1994) shows that the symmetry breaking effects of the shear flow are sufficiently reduced by the splitting apart of the constituent roll modes of hexagonal convection, or indeed any subcritical convection, to take place.

In the first instance we shall in §2 derive the nonlinear ordinary differential equation for the amplitude of single set of roll disturbances in an unsteady flow. The equation is similar to that found for Taylor vortex disturbances in journal bearings by DiPrima & Stuart (1975). Floquet theory is used to discuss the stability properties of the bifurcating finite-amplitude disturbances given in that Section.

In §3 we extend our analysis to derive the coupled evolution equations for all possible roll disturbances. The possible stable finite-amplitude roll modes are determined but our analysis breaks down for modes orientated in a direction close to that of the most dangerous linear mode. A separate analysis is carried out for a three-dimensional packet of modes centred on the most dangerous one. This analysis is also presented in §3 and we obtain a generalization of the Newell–Whitehead (1969) equation which accounts for the effect of a small-amplitude unsteady shear flow. An analysis of the solutions of this equation then determines the possible stable states when the Rayleigh and/or Reynolds numbers are increased slightly beyond their critical values according to linear theory.

In §4 we determine a lower bound for the frequency below which the system behaves in a quasi-steady manner. This is done using the ideas of Hall (1983) and Lettis (1987). The main idea is that, at low enough frequencies, small imperfections in the system can produce the local growth and equilibration to a state anticipated on the basis of a quasi-steady analysis even when an imperfection-free analysis along the lines of Hall (1975) predicts no convection. Finally in Section 5 we will draw some conclusions.

2. The evolution equation for a convection roll in an unsteady shear flow

We consider the flow of a Boussinesq fluid confined between the walls at $z = 0, d$. We suppose that the lower wall has temperature $T_0 + \Delta T$ whereas the upper one has temperature T_0. Furthermore the lower wall has velocities $(\kappa/d)\lambda_1, \cos\omega\tau, (\kappa/d)\lambda_2 \cos[\omega\tau + \gamma]$ in the x- and y-directions. Here we have denoted the thermal diffusivity by κ and τ is a dimensionless time variable scaled on $d^2\kappa^{-1}$. We shall confine our attention to the case $\omega \ll \sigma$, σ being the Prandtl number, so that fluid motion driven by the wall is

quasi-steady. Following Kelly & Hu (1993) and Hall & Kelly (1994) we assume that the flow oscillations are of small amplitude and therefore write

$$\lambda_1 = \hat{\lambda}_1\delta,\ \lambda_2 = \hat{\lambda}_2\delta,\ \omega = \Omega\delta^2,\ t = \delta^2\tau,$$

and then $\hat{\lambda}_1, \hat{\lambda}_2$ and Ω are held fixed in the limit $\delta \to 0$. Throughout this paper we shall scale velocities on κ/d so that for small δ the basic flow is given by

$$\boldsymbol{u} = \delta\{\hat{\lambda}_1 \cos\Omega t, \hat{\lambda}_2 \cos[\Omega t + \gamma], 0\}(1 - z) + O(\delta^3).$$

The basic temperature fluid does not depend on the shear flow and is therefore proportional to the scaled vertical coordinate z. A linear instability analysis shows that the shear flow produces an order-δ^2 correction to the critical Rayleigh number R_c; see Kelly & Hu (1993).

Hall & Kelly investigated the manner in which finite-amplitude hexagonal convection cells occurring in a non-Boussinesq fluid are modified by the shear flow. The latter analysis requires the interaction of a triad of rolls which reinforce each other at quadratic order. Here we restrict our analysis to Boussinesq fluids and small-amplitude shear flows and, as a result of these restrictions, no subcritical bifurcation is possible. For simplicity in the analysis we consider the wall to be driven by a prescribed shear stress and so assume the perturbation shear stress to be zero at both boundaries. Relative to the case of a fixed velocity, we expect the results to be qualitatively correct at low frequencies. In the first instance we shall here consider the nonlinear evolution of a single mode and we seek a finite-amplitude solution with R differing from its critical value $R_c = 27\pi^4/4$ by $O(\delta^2)$. We therefore write

$$R = R_c + \delta^2\hat{R}_2 + \ldots,$$

and expand, for example, the perturbed normal velocity in the form

$$w = \frac{3\pi^2}{2}\delta X(t)\sin\pi z \exp \mathrm{i}\left\{k_x\left[x - \frac{\hat{\lambda}_1 \sin\Omega t}{2\delta\Omega}\right] + k_y\left[y - \frac{\hat{\lambda}_2 \sin(\Omega t + \gamma)}{2\delta\Omega}\right]\right\} + \text{complex conjugate.} \tag{2.1}$$

Here the time-dependent term in the exponential factor has been inserted in order that the order-δ^2 solvability condition is automatically satisfied. At cubic order, by use of a similar condition, we find that the amplitude function $X(t)$ satisfies the equation

$$\frac{\mathrm{d}X}{\mathrm{d}t} = \mu\left\{\hat{R}_2 - \lambda^* G^2(t)\right\}X - \alpha X|X|^2, \tag{2.2}$$

where

$$G(t) = \hat{\lambda}_1 \cos\theta \cos\Omega t + \hat{\lambda}_2 \sin\theta \cos(\Omega t + \gamma), \tag{2.3a}$$

with

$$\theta = \tan^{-1}\frac{k_y}{k_x},\ \alpha = \frac{\sigma}{8(1+\sigma)}, \tag{2.3b}$$

and the constants λ^*, μ are as defined by Hall & Kelly (1994).

If we ignore the nonlinear term in (2.2) we can integrate to find the change in X over one period; the flow is then found to be neutrally stable at $\hat{R}_2 = R_2(\theta)$ when

$$R_2(\theta) = \frac{\lambda^*}{2}\left\{\hat{\lambda}_1^2 \cos^2\theta + \hat{\lambda}_2^2 \sin^2\theta + 2\hat{\lambda}_1\hat{\lambda}_2 \sin\theta\cos\theta\cos\gamma\right\}. \tag{2.4}$$

The constant λ^* is always positive so that $R_2(\theta)$ is also positive for $\hat{\lambda}_1, \hat{\lambda}_2 > 0$, and the flow oscillations have a stabilizing effect on the convection. In general $R_2(\theta)$ has a minimum for each value of $(\hat{\lambda}_1, \hat{\lambda}_2, \gamma)$ so that there is a linear selection process to determine the orientation of the first roll mode to be excited. Here we shall investigate the role of nonlinear effects in the selection mechanism.

An important result found by Kelly & Hu (1993) is that the stabilizing effect is a maximum in the limit of zero frequency for the case of one wall oscillating and with $\sigma > 2$. At low frequencies intuition leads us to expect that a quasi-steady response of the fluid should occur with the rolls being in the direction of the shear so that $R_2 = 0$. However (2.4) is not consistent with the result of a quasi-steady instability analysis based on the instantaneous profile. Therefore some further analysis must be carried out. In fact a similar inconsistency between theory (both linear and nonlinear) and physical intuition was found for the modulated Taylor vortex problem by Hall (1975). The reconciliation of theory with what we expect the fluid response to be at low frequencies was first given by Lettis (1987). Essentially it turns out that the theory only holds until the modulation is slow enough for a disturbance to amplify from an imperfection in the system whenever the flow is instantaneously unstable. The same mechanism will be shown to be crucial in the problem considered here. Before going on, it should be noted that for this particular flow, axes can be defined in the quasi-steady limit that are aligned with the shear. For more general basic flows, such axes might not exist, and so stabilization can then be obtained as $\Omega \to 0$.

The finite-amplitude solution and its stability

The coefficients of (2.2) are real so that, following DiPrima & Stuart (1975), without any loss of generality we can take X to be real and integrate to find the periodic solution

$$X^{-2} = X_0^{-2}(t) = \frac{2\alpha}{I}\left\{\int_0^t I\,\mathrm{d}t + \frac{\int_0^{2\pi/\Omega} I\,\mathrm{d}t}{I(2\pi/\Omega) - 1}\right\}, \tag{2.5}$$

with $I(t) = \exp\{2\mu\int_0^t[-\lambda^* G^2 + \hat{R}_2]\}\mathrm{d}t$.

It is easy to see from (2.2) that this solution exists for $\hat{R}_2 > R_2(\theta)$ since, if we divide by X and integrate over a period, we find that

$$\alpha\int_0^{2\pi/\Omega} |X|^2\mathrm{d}t = \mu 2\pi/\Omega\left\{\hat{R}_2 - R_2(\theta)\right\}. \tag{2.6}$$

Thus the mean value of $|X|^2$ over a period is related to the degree of supercriticality in an identical way to the unmodulated case so the only effect of the modulation is to push the bifurcation point to a higher Rayleigh number. In order to consider the possible instability of (2.5) we write

$$X = X_0 + \tilde{X}_r(t) + \mathrm{i}\tilde{X}_i(t)$$

with $|\tilde{X}| \ll |X_0|$ and substitution into (2.2) yields uncoupled linear equations for $\tilde{X}_r$ and $\tilde{X}_i$ which have solutions such that

$$\frac{X_r(2\pi)}{X_r(0)} = \mathrm{e}^{-2\mu(\hat{R}_2 - R_2(\theta))}, \quad \frac{X_i(2\pi)}{X_i(0)} = 1.$$

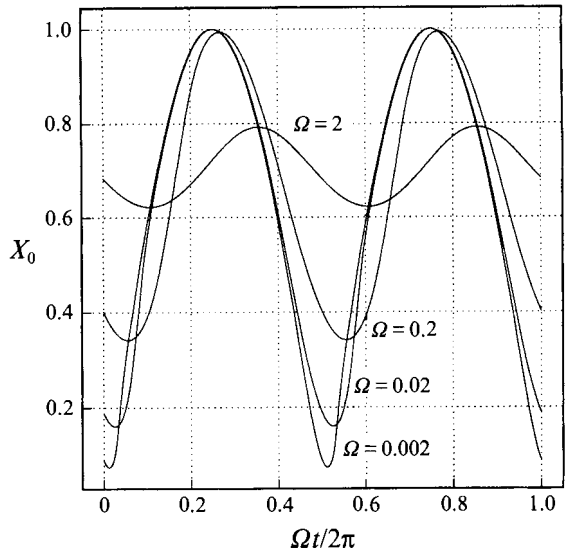

FIGURE 1. The periodic solution (2.5) for $\sigma = 1, \lambda^* = 1, \hat{\lambda}_1 = 1, \hat{\lambda}_2 = 2$ and $\Omega = 0.002, 0.02, 0.2, 2$.

Thus the disturbance $\pi/2$ radians out of phase with $X = X_0$ is neutrally stable whereas the in-phase mode is stable. This is the usual result for the Bénard problem, so that the only effect of the oscillations is indeed to push the bifurcation point to a higher Rayleigh number.

In order to see how the solution (2.5) changes when the frequency Ω is altered let us now focus on, for example, the particular case with say $\sigma = 1, \gamma = \pi/2, \hat{R}_2 = 1, \lambda^* = 1$. The most dangerous mode cannot be identified until the ratio $\hat{\lambda}_2/\hat{\lambda}_1$ is specified therefore, as a typical example, we take $\hat{\lambda}_1 = 1, \hat{\lambda}_2 = 2$. In this case the most dangerous mode corresponds to $\theta = 0$ so that the rolls are aligned with the direction of maximum shear.

Figure 1 shows the solution $X_0(t)$ for a variety of frequencies for the above case. We see that the amplitude becomes progressively concentrated about the times when $G = 0$ as Ω gets smaller. This result is not surprising since, on the basis of a quasi-steady linear theory, the most unstable times correspond to $\Omega t = \pi/2, 3\pi/2, \ldots$.

3. The amplitude equations for interacting rolls

The work of Kelly & Hu (1993) showed that an unsteady non-planar shear flow selects a particular roll orientation which amplifies first. The discussion of the previous section shows that every possible streamwise roll bifurcates supercritically from its critical linear value and is stable to rolls of the same orientation and wavenumber as that of the bifurcating mode. Now we shall extend the analysis to account for interactions between rolls of different orientations so as to allow the pattern to adjust to the changing shear. In order to do so we replace (2.1) by

$$w = \frac{3\pi^2}{2}\delta \sin \pi z \sum_{n=1}^{N} X_n(t) \exp \frac{\mathrm{i}\pi}{\sqrt{2}} \left\{ \cos\theta_n \left[x - \frac{\hat{\lambda}_1 \sin \Omega t}{2\delta\Omega} \right] + \sin\theta_n \left[y - \frac{\hat{\lambda}_2 \sin(\Omega t + \gamma)}{2\delta\Omega} \right] \right\} + \text{complex conjugate} + \ldots, \tag{3.1}$$

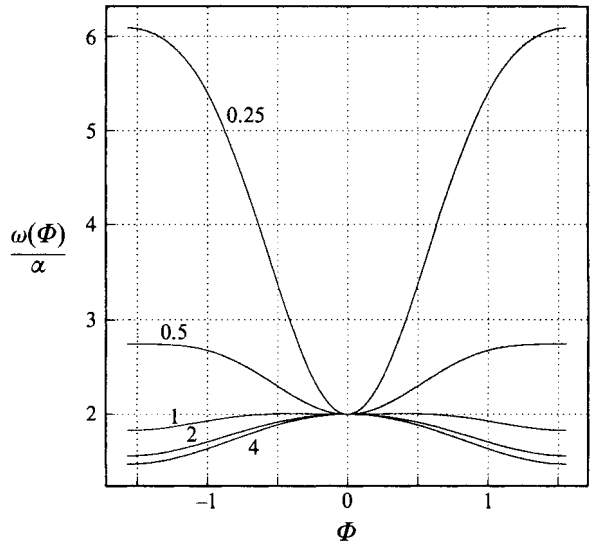

FIGURE 2. The nonlinear interaction coefficient $\omega(\Phi)/\alpha, -\pi/2 < \Phi < \pi/2$, for $\sigma = 0.25, 0.5, 1, 2, 4$.

where $-\pi/2 \leqslant \theta_1 < \theta_2 < \ldots < \theta_N < \pi/2$ for some value of $N \geqslant 1$. We note here that, on the basis of linear theory, the nth mode is unstable when

$$R > R_c + \delta^2 R_2(\theta_n) + \ldots, \tag{3.2}$$

so that the modes in general bifurcate at different values of the Rayleigh number. It is this fact that Hall & Kelly (1994) found was sufficient to destroy the possibility of hexagonal cells which usually occur when the variation with temperature of fluid properties is taken into account. In fact, since hexagons are associated with the breaking of symmetry about the plane $z = \frac{1}{2}$, we should not expect them to occur here. At order δ^3 we find that the amplitude equation to determine $X_n(t)$ is

$$\frac{\mathrm{d}X_n}{\mathrm{d}t} = \mu\left\{\hat{R}_2 - \lambda^* G^2(\theta_n, t)\right\} X_n(t) - \sum_{m=1}^{N} \omega_{mn} X_n |X_m|^2. \tag{3.3}$$

Here the function G is defined by (2.3a) whilst the interaction coefficient $\omega_{mn}, m, n = 1 \ldots N$ can be written down in closed (but tedious) form. It suffices here to note that $\omega_{mn} \geqslant \omega_{nn} = \alpha$ for all m and n with equality only if $m = n$. In addition it is easy to show that $\omega_{mn} = \omega_{nm}$ and that

$$\omega_{mn} = \omega(|\theta_m - \theta_n|)$$

so that the interaction coefficients for a pair of rolls is a function only of the angle between the rolls. In figure 2 we show $\omega(\Phi)/\alpha$ for $0 < \Phi < \pi$ for a range of Prandt numbers. Now suppose that we consider the finite-amplitude disturbance with $X_n = 0, n \neq \bar{n}$ and $X_{\bar{n}}$ given by the periodic solution of (3.3) with $n = \bar{n}$. Thus $X_{\bar{n}}$ is given by (2.5) with $G = G(\theta_{\bar{n}}, t)$ and we now look at the possible instability of this mode to a roll inclined at a finite angle to it.

It follows that the linearized amplitude equation for the nth mode has exponential solutions with growth rate σ_L given by

$$\sigma_L = \left\{\hat{R}_2 - R_2(\theta_n) - \frac{\omega_{n\bar{n}}}{\alpha}[\hat{R}_2 - R_2(\theta_{\bar{n}})]\right\} \tag{3.4}$$

and we note from figure 2 that $\omega_{n\bar{n}}/\alpha$ is always greater than unity whilst if $n = \bar{n}$ (2.16) is recovered. We can then immediately deduce the following results from (3.4).

(*a*) If the $\bar{n}$ mode is the most dangerous mode on the basis of linear theory then this mode is stable to all small-amplitude rolls inclined at any angle to the $\theta_{\bar{n}}$-direction.

(*b*) If the $\bar{n}$ mode is not the most unstable mode then it is stable to all linearly more stable modes. It is unstable over a finite range of values of $\hat{R}_2$, beginning at $\hat{R}_2 = R_2(\theta_{\bar{n}})$, to rolls more unstable on the basis of linear theory.

Hence the first mode to bifurcate is stable at all supercritical values of $\hat{R}_2$. Thus in any experiment where the Rayleigh number is slowly increased only the mode selected by linear theory will be observed.

Now let us examine in more detail the nature of the secondary bifurcation from a pure mode. In particular we consider the reduced interaction with only the nth and $\bar{n}$th modes present. If we define

$$\frac{2\pi}{\Omega}Q_{\bar{n}} = \int_0^{2\pi/\Omega} |X_{\bar{n}}|^2 \mathrm{d}t, \quad \frac{2\pi}{\Omega}Q_n = \int_0^{2\pi/\Omega} |X_n|^2 \mathrm{d}t,$$

then, after dividing the reduced version of (3.3) through by X_n and $X_{\bar{n}}$ and integrating over a period, we can show that

$$(\bar{\omega}^2 - 1)Q_{\bar{n}} = \frac{\mu}{\alpha}\left\{\hat{R}_2(\bar{\omega} - 1) - \bar{\omega}R_2(\theta_n) + R_2(\theta_{\bar{n}})\right\}, \tag{3.5a}$$

$$(\bar{\omega}^2 - 1)Q_n = \frac{\mu}{\alpha}\left\{\hat{R}_2(\bar{\omega} - 1) - \bar{\omega}R_2(\theta_{\bar{n}}) + R_2(\theta_n)\right\}, \tag{3.5b}$$

where $\alpha\bar{\omega} = \omega(\theta_m - \theta_{\bar{n}})$. Since $Q_n, Q_{\bar{n}}$ are necessarily positive, the finite-amplitude mixed mode given above bifurcates supercritically from the pure $X_{\bar{n}} \neq 0$ mode when

$$\hat{R}_2 = \hat{R}_{2c} = \frac{\bar{\omega}R_2(\theta_{\bar{n}}) - R_2(\theta)}{\bar{\omega} - 1}. \tag{3.6}$$

The mixed mode exists for all $\hat{R}_2 > \hat{R}_{2c}$ and a stability analysis shows that it is always unstable. However the pure mode $X_{\bar{n}} \neq 0$ is made stable after the secondary bifurcation has occurred. The bifurcation picture for the two-mode interaction is then as shown in figure 3. Thus, in an experiment where all modes except two are somehow suppressed, there are two possible stable states at high enough values of the Rayleigh number. However it is unlikely that such an experiment could be carried out so we now see how the bifurcation picture of figure 3 changes when disturbances of any orientation are taken into account. If it turns out that $\hat{R}_{2c}$ is bounded from above when n varies over all the possible modes which are more linearly unstable than the $\bar{n}$th mode, then we can expect multiple steady states at high enough Rayleigh numbers.

An investigation of the behaviour of the different bifurcation points shows that this is indeed the case and that the locus of the points in the (R_2, θ)-plane separating regions of stability and instability on a nonlinear basis is as shown in figure 4 for the case $\tilde{\lambda}_1 = 1, \tilde{\lambda}_2 = 2$. If we choose a roll with a fixed value of θ then the roll is linearly unstable when the continuous curve is crossed. However the finite-amplitude roll which bifurcates from the continuous curve is unstable until the dashed curve is crossed. We also note that the curves touch at $\theta = \theta^* = 0$, which corresponds to the most unstable roll on the basis of linear theory. Actually our expansion procedure fails sufficiently close to θ^* because the bifurcating mode and the neighbouring ones controlling its stability have almost the same orientation and some of the cubic terms not contributing to the amplitude equation become singular; see Newell & Whitehead (1969) for a discussion of this point. The remedy for this difficulty is to look for an

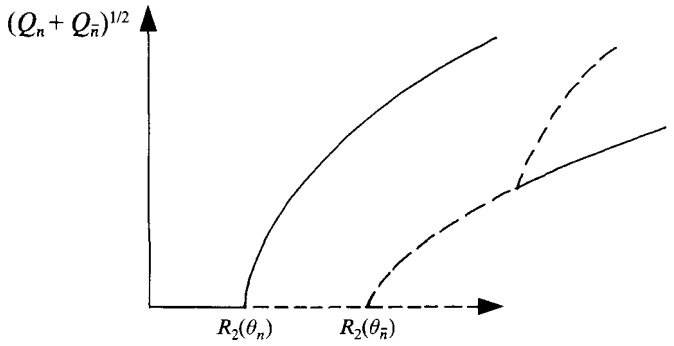

FIGURE 3. The bifurcation picture associated with (3.3) for the case of two modes. Unstable solutions are denoted by the dashed curves.

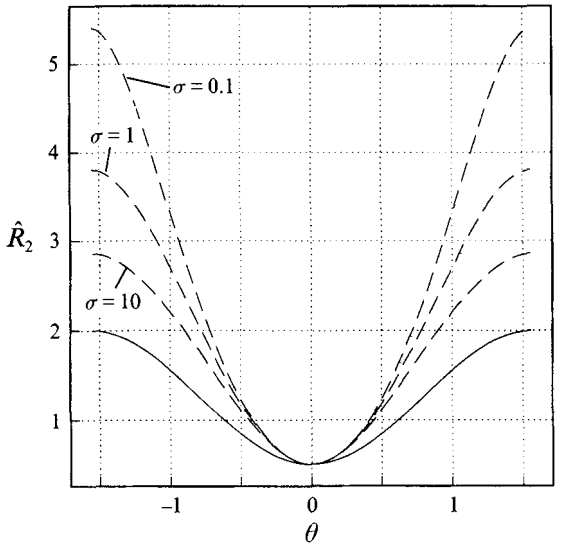

FIGURE 4. The linear and nonlinear stability boundaries for the pure mode periodic solutions of (3.3). The lower curve, $\hat{R}_2 = R_2(\theta)$, determines the value of $\hat{R}_2$ at which the pure mode with the given value of θ bifurcates supercritically from the zero solution. The dashed curves, shown for $\sigma = 0.1, 1, 10$, determine the values of $\hat{R}_2$ above which the bifurcating periodic solution at the given value of θ is stable against all perturbations.

evolution equation for a packet of modes centred on $\theta = \theta^*$. In order to derive the required evolution equation we first consider the linearized amplitude equation obtained from (2.2) by replacing $\cos\theta$ by $(\sqrt{2}/i\pi)\partial/\partial x$ and $\sin\theta$ by $(\sqrt{2}/i\pi)\partial/\partial y$; this gives

$$\frac{\partial X}{\partial t} = \mu\left\{\hat{R}_2 + 2\frac{\lambda^*}{\pi^2}\left[\hat{\lambda}_1 \cos\Omega t\frac{\partial}{\partial x} + \hat{\lambda}_2 \cos(\Omega t + \gamma)\frac{\partial}{\partial y}\right]^2\right\} X. \tag{3.7}$$

where we now think of X as being a function of (t, x, y).

The angle θ^* which determines the orientation of the most dangerous mode selected by linear theory is given by the solution of

$$\int_0^{2\pi/\Omega} G(\theta^*, t)\frac{\partial G}{\partial \theta}(\theta^*, t)\mathrm{d}t = 0 \tag{3.8}$$

because the neutral value of $\hat{R}_2 = R_2(\theta^*) = \lambda^*(\Omega/2\pi)\int_0^{2\pi/\Omega} G^2(\theta^*,t)\mathrm{d}t$. At this stage it is convenient to rotate the x, y-axes so that the x-axis coincides with the θ^* direction. We must then replace (3.7) by

$$\frac{\partial X}{\partial t} = \mu\left\{\hat{R}_2 + \frac{2\lambda^*}{\pi^2}\left[G(\theta^*,t)\frac{\partial}{\partial x} + \frac{\partial G}{\partial \theta^*}(\theta^*,t)\frac{\partial}{\partial y}\right]^2\right\}X. \tag{3.9}$$

Now we introduce the small parameter ϵ by writing

$$\hat{R}_2 = R_2(\theta^*) + \epsilon^2\tilde{R}_2 + \ldots,$$

and introduce new variables ξ, η and T defined by

$$\xi = \epsilon^2 x,\ \eta = \epsilon y,\ T = \epsilon^2 t.$$

In (3.9) we must then replace $\partial/\partial x$ and $\partial/\partial y$ by $\mathrm{i}\pi/\sqrt{2}+\epsilon^2\partial/\delta\xi$ and $\epsilon\partial/\partial\eta$ respectively whilst $\partial/\partial t$ is replaced by $\partial/\partial t + \epsilon^2\partial/\partial T$. If we now expand X in the form

$$X = \tilde{X}_0(\xi,\eta,T,t) + \epsilon\tilde{X}_1(\xi,\eta,T,t) + \ldots$$

and substitute into (3.9) we obtain

$$\frac{\partial\tilde{X}_0}{\partial t} = \mu\left\{R_2(\theta^*) - \lambda^* G^2(\theta^*,t)\right\}\tilde{X}_0,$$

which has the periodic solution

$$\begin{aligned}\tilde{X}_0 &= X_0(\xi,\eta,T)\exp\left[\mu\{R_2(\theta^*)t - \lambda^*\int_0^t G^2(\theta^*,t)\mathrm{d}t\}\right]\\ &= X_0(\xi,\eta,T)E(t),\end{aligned} \tag{3.10}$$

where the periodicity of E follows from the definition of $R_2(\theta^*)$ and X_0 is to be determined at higher order. At order ϵ we find that $\tilde{X}_1$ satisfies an inhomogeneous form of the equation for $\tilde{X}_0$; the solution of that equation may be written in the form

$$\tilde{X}_1 = \frac{\mu\lambda^* 2\sqrt{2}}{\pi}EX_{0\eta}\int_0^t GG_\theta\mathrm{d}t,$$

and the periodicity of $\tilde{X}_1$ in t then follows from (3.8).

At order ϵ^2 we find that the equation for X_2 is forced by both the order-ϵ^0, ϵ solutions and has a solution periodic in t if

$$\frac{\partial X_0}{\partial T} = \mu\tilde{R}_2 X_0 + \frac{2\sqrt{2}}{\pi}R_2^*\mu\lambda^*\left\{\mathrm{i}\frac{\partial}{\partial\xi} + \tilde{\omega}\frac{\partial^2}{\partial\eta^2}\right\}X_0. \tag{3.11}$$

Here $R_2^* = R_2(\theta^*)$ and the positive constant $\tilde{\omega}$ is defined by the equation

$$\pi\sqrt{2}\tilde{\omega} = \int_0^{2\pi/\Omega} G_\theta^2\mathrm{d}t \Big/ \int_0^{2\pi/\Omega} G^2\mathrm{d}t, \tag{3.12}$$

evaluated at $\theta = \theta^*$. The operator $\{\mathrm{i}\partial/\partial\xi + \tilde{\omega}\partial^2/\partial\eta^2\}$ leads to a negative contribution to the growth rate when we seek a solution periodic in ξ and η, since k_1 and k_2, the ξ and η wavenumbers, must be related by $2k_1 = -k_2^2$ if the roll is to have wavenumber $\pi/\sqrt{2}$ up to order ϵ^2. Equation (3.11) therefore leads to the eigenrelation for a roll almost parallel with the (rotated) x-direction. The equation is valid for $\epsilon \gg \delta$, since when $\epsilon \sim \delta$ further terms, essentially due to the expansion of $\partial^2/\partial x^2 + \partial^2/\partial y^2$ in terms of the new variables, come into play; see Newell & Whitehead (1969). Thus

for completeness we now take $\epsilon = \delta$. If we now write the eigenrelation for Bénard convection without a shear flow in the form

$$\left(\frac{3\pi^2}{2} - \epsilon^2\mathscr{L} + \frac{\epsilon^2}{\sigma}\frac{\partial}{\partial T}\right)\left(\frac{3\pi^2}{2} - \epsilon^2\mathscr{L} + \epsilon^2\frac{\partial}{\partial T}\right)\left(\frac{3\pi^2}{2} - \epsilon^2\mathscr{L}\right) \equiv \frac{+\pi^2}{2}\epsilon^2\tilde{R}_2 + \frac{27\pi^6}{8} - \frac{27\pi^4}{4}\epsilon^2\mathscr{L}$$

with $\mathscr{L} \equiv \sqrt{2}\pi i\partial_\xi + \partial_\eta^2 + \epsilon^2\partial_\xi^2$, and expand in powers of ϵ we deduce that, when $\epsilon = \delta$, equation (3.11) must be modified to give

$$\frac{\partial X_0}{\partial T} = \mu\tilde{R}_2 X_0 + \frac{2\sqrt{2}}{\pi}R_2^*\mu\lambda^*\left\{i\frac{\partial}{\partial\xi} + \tilde{\omega}\frac{\partial^2}{\partial\eta^2}\right\}X_0 - \frac{4}{1+1/\sigma}\left\{i\frac{\partial}{\partial\xi} + \frac{1}{\pi\sqrt{2}}\frac{\partial^2}{\partial\eta^2}\right\}^2 X_0. \tag{3.13}$$

Now suppose that we retain nonlinear effects in the analysis leading to (3.13); this is most easily done by inserting the term $-\alpha X|X|^2$ on the right-hand side of equation (3.9). Note that this is formally valid only at infinite Prandtl numbers where we can ignore the mean flow correction to the velocity field; see Newell & Whitehead (1969) and Siggia & Zippelius (1981).

The appropriate nonlinear form of (3.13) is then found to be

$$\frac{\partial X_0}{\partial T} = \mu\tilde{R}_2 X_0 + \frac{2\sqrt{2}}{\pi}R_2^*\mu\lambda^*\left\{i\frac{\partial}{\partial\xi} + \tilde{\omega}\frac{\partial^2}{\partial\eta^2}\right\}X_0 - 4\left\{i\frac{\partial}{\partial\xi} + \frac{1}{\pi\sqrt{2}}\frac{\partial^2}{\partial\eta^2}\right\}^2 X_0 - \tilde{\alpha}X_0|X_0|^2, \tag{3.14}$$

where

$$\tilde{\alpha} = \frac{\alpha\Omega}{2\pi}\int_0^{2\pi/\Omega} E^2(t)\mathrm{d}t,$$

and R_2^*, μ are evaluated at infinite Prandtl number.

If we linearize (3.14) it is easy to show that, on the basis of linear theory, exponentially growing solutions will occur when

$$\tilde{R}_2 > \tilde{R}_{2c} = \frac{\mu R_2^{*2}\lambda^{*2}}{2\pi^2}.$$

If we assume that $\tilde{R}_2 > \tilde{R}_{2c}$, and note that $\tilde{\alpha}, \mu$ are positive, then a more convenient form of (3.14) can be obtained by writing

$$2\bar{\xi} = [\mu(\tilde{R}_2 - \tilde{R}_{2c})]^{1/2}\xi, \quad 2^{1/4}\bar{\eta} = [\mu\pi^2(\tilde{R}_2 - \tilde{R}_{2c})]^{1/4}\eta, \tag{3.15a}$$

$$\bar{X} = \left[\frac{\mu(\tilde{R}_2 - \tilde{R}_{2c})}{\tilde{\alpha}}\right]^{1/2} X_0 \exp\left\{\frac{-i}{2\pi\sqrt{2}}R_2^*\mu\lambda^*\xi\right\}, \tag{3.15b}$$

$$\bar{T} = \mu(\tilde{R}_2 - \tilde{R}_{2c})T, \; J^2 = \frac{2R_2^*\mu^{1/2}\lambda^*}{(\tilde{R}_2 - \tilde{R}_{2c})^{1/2}}\left(\tilde{\omega} - \frac{1}{\pi\sqrt{2}}\right). \tag{3.15c}$$

We note that J^2 is positive.

Equation (3.13) can then be written in the form

$$\frac{\partial\bar{X}}{\partial\bar{T}} = \bar{X}[1 - |\bar{X}|^2] + J^2\frac{\partial^2\bar{X}}{\partial\bar{\eta}^2} - \left\{i\frac{\partial}{\partial\bar{\xi}} + \frac{\partial^2}{\partial\bar{\eta}^2}\right\}^2\bar{X}. \tag{3.16}$$

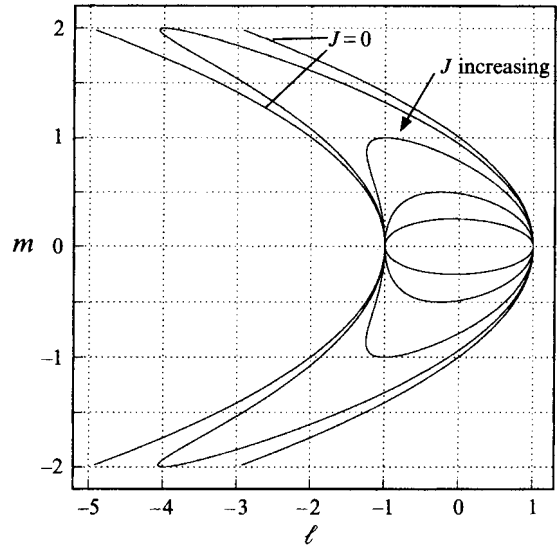

FIGURE 5. The regions of existence of the solution (3.17) for $J = 0, 0.5, 1, 2, 4$. For $J = 0$ the solution exists between the two curves labelled $J = 0$. For non-zero values of J the solution exists within the closed curves.

We can think of J in the above equation as a scaled Reynolds number and setting $J = 0$ we recover a scaled form of the Newell–Whitehead equation. We note further that (3.16) also applies to the case of a steady shear flow but we cannot find a reference to it in the literature.

Now let us consider the nature of the solutions of (3.16) and their stability characteristics. In the first instance we note that (3.16) has plane wave solutions of the form

$$\overline{X} = p\mathrm{e}^{\mathrm{i}\{\ell\bar{\xi}+m\bar{\eta}\}}, \quad p^2 = 1 - J^2m^2 - (\ell + m^2)^2. \tag{3.17}$$

The above solution exists only for $1 \geqslant J^2m^2 + (\ell + m^2)^2$ and in figure 5 we show a plot in the (ℓ, m)-plane of the region where it exists for different values of the scaled Reynolds number J. It can be seen that increasing J causes the region to contract in size. We further note that increasing J in this manner corresponds to increasing the flow Reynolds number with the Rayleigh number held fixed. In order to study the stability properties of (3.17) we write

$$\overline{X} = p\mathrm{e}^{\mathrm{i}\{\ell\bar{\xi}+m\bar{\eta}\}} + a\mathrm{e}^{\mathrm{i}\{[\ell+\mu]\bar{\xi}+[m+\nu]\bar{\eta}\}} + b\mathrm{e}^{\mathrm{i}\{[\ell-\mu]\bar{\xi}+[m-\nu]\bar{\eta}\}}$$

where $|a| \ll 1, |b| \ll 1$. We can then substitute into (3.16) to obtain a pair of coupled ordinary differential equations in $\overline{T}$ which allow exponentially growing solutions with $a, \bar{b} \sim \mathrm{e}^{\bar{\gamma}\overline{T}}$ where the growth rate $\bar{\gamma}$ is determined by

$$\bar{\gamma} = -p^2 - (\nu^4 + 6m^2\nu^2 + 2\ell\nu^2 + 4m\mu\nu + \mu^2) - J^2\nu^2 + [p^4 + (2[\mu + 2m\nu][\ell + m^2 + \nu^2] + 2J^2m\nu)^2]^{1/2}. \tag{3.18}$$

Following Newell & Whitehead it is easy to show that for the zero shear case, i.e. $J = 0$, the two most unstable disturbances correspond to rolls parallel and perpendicular to the given finite-amplitude roll state. More precisely we find that,

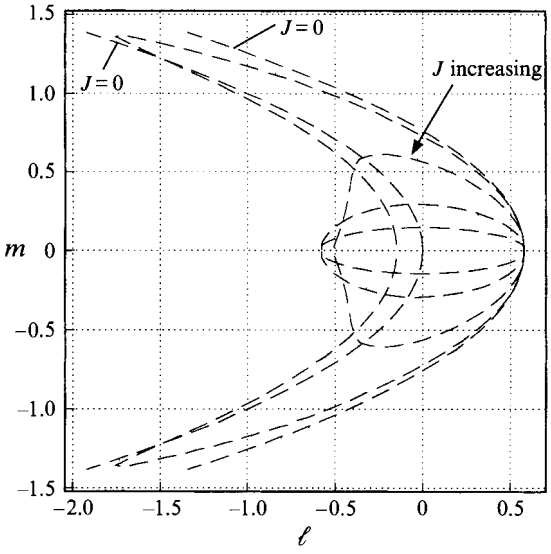

FIGURE 6. The regions of stability of the solution (3.17) for $J = 0, 0.5, 1, 2, 4$. For $J = 0$ the solution is stable between the two curves labelled $J = 0$. For non-zero values of J the solutions are stable within the closed curves.

for $J = 0$, the finite-amplitude state (3.17) is unstable to a perpendicular set of rolls whenever $\ell + m^2 < 0$ and unstable to parallel rolls whenever $|\ell + m^2| > 1/\sqrt{3}$. The latter stability boundary corresponds to the Eckhaus instability mechanism and we deduce that (3.17) is stable only in the regime

$$0 < \ell + m^2 < \frac{1}{\sqrt{3}}. \tag{3.19}$$

When $J \neq 0$ we cannot write down an analytical expansion for the stability boundary but it is a straightforward numerical task to derive the stability boundaries numerically from (3.18). The results are illustrated in figure 6 for the range of values of the shear corresponding to figure 5. We see that the shear stabilizes a small band of modes with $\ell + m^2 < 0$. However, we see that as the shear increases, the region where stable modes exist shrinks, and in fact becomes vanishingly small when $J \to \infty$. We are now in a position to describe the evolution of the most dangerous mode according to linear theory.

Firstly let us consider the implications of the results of figures 5 and 6 in more detail. In particular we concern ourselves with the implications for any experimental investigation of the problem discussed here and the implications for the linear roll mode selection problem of Kelly & Hu (1993). We first remind the reader about the zero shear flow case $J = 0$. In this case stable solutions occur between the curves $\ell + m^2 = 0, 1/\sqrt{3}$. Suppose that a solution has been established at some values of $\Delta\tilde{R}_2 = (\tilde{R}_2 - \tilde{R}_{2c})$ with $\ell = \bar{\ell}, m = \bar{m}$ and that $\Delta\tilde{R}_2$ is then varied slowly keeping the physical wavelength of the roll constant. In view of (3.15a) this means that when $\Delta\tilde{R}_2$ varies (ℓ, m) must move along the parabola $\ell = \bar{\ell} m^2/\bar{m}^2$. If $\Delta\tilde{R}_2$ is an increasing function ℓ and m move towards the origin, otherwise ℓ and m move towards infinity. It follows that when $\Delta\tilde{R}_2$ increases the roll pattern remains stable whilst if $\Delta\tilde{R}_2$ decreases the given roll pattern becomes unstable when $(\bar{\ell}/\bar{m}^2 + 1)\, m^2 = 1/\sqrt{3}$. Thus for the

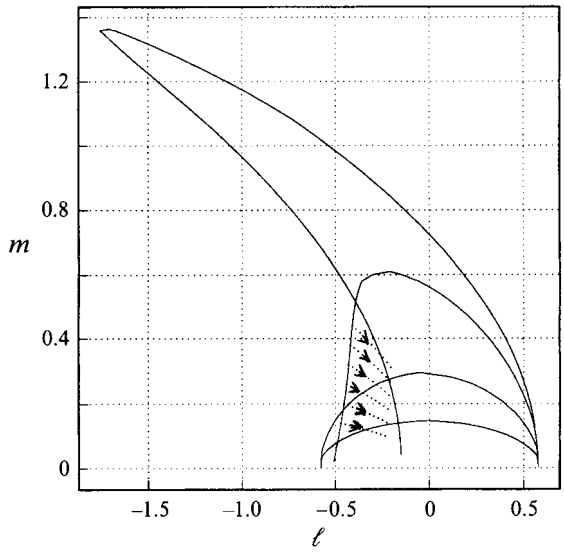

FIGURE 7. The upper part of figure 6 with the dotted curves representing the paths taken by the wavenumber when the Rayleigh number is increased.

zero shear case any given roll pattern except that with $\bar{\ell} = \bar{m} = 0$ becomes unstable at a critical value of $\Delta\tilde{R}_2$ when the latter quantity is decreased.

We now suppose that $J \neq 0$ and see how the above picture is changed. Firstly we suppose that the shear flow amplitude is held fixed whilst the Rayleigh number is varied. Consider then the stability of the roll which initially exists for say $J = \bar{J}, \ell = \bar{\ell}, m = \bar{m}$. Thus for a given $\bar{J}$ the point $(\bar{\ell}, \bar{m})$ is within the appropriate closed curve of the type shown in figure 6. When $\Delta\tilde{R}_2$ is varied the fixed-wavelength roll is once again tracked by moving along the parabola $\ell = \bar{\ell}m^2/\bar{m}^2$, either towards or away from the origin depending on whether $\Delta\tilde{R}_2$ is increasing or decreasing. From the definition of J^2, (3.15*c*), it follows that when $\Delta\hat{R}_2$ varies by a factor $\bar{A} > 0$ then the stable region for the roll now corresponds to that for $J = \bar{J}/\bar{A}^{1/2}$. Thus as the point (ℓ, m) moves along the parabola $\ell = \bar{\ell}m^2/\bar{m}^2$ the appropriate stability region is that computed with $J = \bar{J}\left(\ell/\bar{\ell}\right)^{1/2}$. It is easy to see from figure 6 that this means that any mode with $\bar{\ell}$ or $\bar{m} \neq 0$ will become unstable for sufficiently small $\Delta\tilde{R}_2$. When $\Delta\tilde{R}_2$ is an increasing function the situation is more complex but in most cases a given roll remains stable whilst $\Delta\tilde{R}_2$ increases to infinity. However, for some $\bar{J}$ this is not the case; in particular there is a range of values of $\bar{J}$ around $\bar{J} = 1$ where some modes become unstable with increasing $\Delta\tilde{R}_2$. We refer to figure 7 where we have shown the upper part of figure 6 in more detail. The dotted curve show the path taken by the point (ℓ, m) for different initial values on the limit of the stability region for the $J = 1$ case. The arrows correspond to the direction to be followed when the Rayleigh number is increased. The other end points of the curves correspond to the Rayleigh number difference being increased by a factor of 4. Thus at the end points of each dotted curve the stability region of the mode is governed by the $J = \frac{1}{2}$ case. We see that the four lower modes have therefore passed into an unstable region and therefore the flow pattern will change. Thus in the presence of an unsteady shear flow roll patterns can be destroyed in some cases by increasing the Rayleigh number.

Next suppose that the Rayleigh number is held fixed and the shear flow amplitude is varied. In fact since the Rayleigh number has been expanded in the form

$$R = \frac{27\pi^4}{4} + R_2^*\epsilon^2 + \epsilon^4\tilde{R}_2 + \cdots$$

and R_2^* is proportional to the square of the shear flow amplitude then varying the amplitude by $O(1)$ will alter the order-ϵ^2 terms above and our expansion will fail unless we perturb R_2^* only by $O(\epsilon^2)$. This means that our previous analysis is valid so long as we replace $\tilde{R}_2$ by $\tilde{R}_2 + \epsilon^4(R_2^* - R_2^{**})$ where R_2^{**} is R_2^* evaluated at a fixed value of $(\hat{\lambda}_1, \hat{\lambda}_2)$. Thus we return to the problem of fixed shear flow amplitude and varying Rayleigh number and our previous discussion then applies. Hence if the shear flow amplitude is increased eventually all modes except the one with $\bar{\ell} = \bar{m} = 0$ will become unstable whilst some rolls can be destabilized with decreasing shear flow amplitude.

4. The quasi-steady limit of the amplitude equations

In §3 we discussed the solution of the coupled amplitude equations given by (3.3). That discussion was restricted to the interaction of a pair of modes and we found that, for a given value of θ, there exists a critical value of $\hat{R}_2 = \hat{R}_{2c}$, greater than the linear critical value of the mode in question, above which the mode is stable to all other perturbations. Figure 3 illustrated the latter result and shows that, with θ and σ fixed, linear instability theory predicts the onset of convection when the lower curve is crossed, whilst nonlinear theory shows that the resulting finite-amplitude disturbance is stable only beyond the dashed curve. The situation when $\theta = \theta^*$, the orientation of the most dangerous mode of linear theory, was discussed as a special case at the end of the last Section.

We shall now discuss the solution of (3.3) in the low-frequency limit $\Omega \to 0$. More precisely we shall determine the size of the frequency below which imperfections present in the system must be allowed for. This problem for a single mode was first discussed by Lettis (1987) using the ideas of Hall (1983) and subsequently by Barenghi & Jones (1989) in the context of the Taylor vortex problem. The reason why imperfections are important at low frequencies can be seen from equation (2.2) which shows that a single mode bifurcates supercritically from $\hat{R}_2 = R_2(\theta)$ where R_2 is the neutral value of $\hat{R}_2$ predicted by linear theory. At low frequencies we expect linear instability to occur whenever the coefficient $(\hat{R}_2 - \lambda^* G^2)$ in (2.2) is instantaneously positive. The analysis of Lettis (1987) showed clearly how imperfections come into play in order to make theory and physical intuition consistent. In the presence of imperfections and small frequencies we can show from (2.2) that the non-zero solution of this equation grows (locally) exponentially whenever $\hat{R}_2 > \lambda^* G^2$ and decays exponentially otherwise. It turns out that when $\hat{R}_2 < R_2(\theta)$ the exponential decay in the subcritical regimes dominates the growth elsewhere so that the only periodic solution of (2.2) is the zero-amplitude case. The latter result is consistent with (2.6) since, when $\hat{R}_2 > R_2(\theta)$, the growth and decay over different parts of the period balance and a non-zero finite-amplitude state exists. However, the instantaneous amplitude of this finite-amplitude state continues to decay exponentially in the parts of the cycle where $\hat{R}_2 < \lambda^* G^2$ so that the disturbance is concentrated in the supercritical parts of the period, see figure 1. However when $\hat{R}_2 > \lambda^* G^2$ the amplitude is of the same magnitude throughout the period. It is in the regime where $\hat{R}_2 - \lambda^* G^2$ changes sign within a period that imperfections play a crucial role.

Suppose then that the typical size of any imperfections present in the system is $O(\delta^3)$. The imperfections might arise from end effects, Hall & Walton (1978), wall undulations, Kelly & Pal (1978), or random fluctuations within the flow. If we allow the imperfections to vary on the same time scale as the basic flow, then the appropriate generalization of (2.2) is, after some analysis, found to be

$$\frac{\mathrm{d}X}{\mathrm{d}t} = \mu\left\{\hat{R}_2 - \lambda^* G^2(t)\right\} X - \alpha X|X|^2 + \hat{\gamma} I(t). \tag{4.1}$$

Here G is as defined by (2.3*a*), $\hat{\gamma}$ is a scaled $O(1)$ constant and $I(t) = O(1)$ represents the fluctuating imperfection. In general we expect that $I(t)$ will vary on a different time scale than the basic flow but the scale of variation of the imperfection is not crucial to the following discussion. Indeed if the imperfections arise from end effects, Hall & Walton (1978), I is a constant. We now state the main conclusions which can be drawn from Lettis (1987) who discussed an equation similar to (4.1). We consider the limit $\Omega \to 0$ and suppose that $\hat{R}_2 - \lambda^* G^2$ changes sign within a period of oscillation. It turns out that in this limit and with $\hat{\gamma} \sim \Omega^K, K > 0$, there is a non-zero periodic solution of (4.1) with $X = O(1)$ whenever $\hat{R}_2 > \lambda^* G^2$, and $X = O(\hat{\gamma})$ otherwise. The non-zero finite-amplitude solution is made possible by the fact that in the linearly stable part of the cycle the imperfection prevents X from becoming exponentially small. The choice $K = \frac{3}{4}$ is the easiest to describe since in that case all of the terms in (4.1) are comparable at the instant when the modes in question become locally unstable.

The above discussion refers to the case when $\hat{R}_2 - \lambda^* G^2$ changes sign in a period. If $\hat{R}_2$ is decreased the finite-amplitude solutions driven by the imperfections are $O(\hat{\gamma})$ except for smaller and smaller intervals. When $\hat{R}_2 > \lambda^* G^2$ throughout the period the imperfections play no role at leading order and the solution is given by (2.5) together with an $O(\hat{\gamma})$ correction.

Now let us determine the role of imperfections in the solution of (3.3). Again for an imperfection of size $O(\delta^3)$, it can be shown that (3.3) is modified to give

$$\frac{\mathrm{d}X_n}{\mathrm{d}t} = \mu\left\{\hat{R}_2 - \lambda^* G^2\right\} X_n - \sum_{m=1}^{N} \omega_{mn} X_n |X_m|^2 + \gamma_n I_n(t). \tag{4.2}$$

Here γ_n for $n = 1, 2, \ldots$ are scaled constants and $I_n = O(1)$ determines the time variation of the imperfection of the nth mode. Note also that there is no physical mechanism to select which of the N modes should dominate the interaction. Some discussion of equations of the type (4.2) is given in Benoit (1990); see for example the paper by Erneux *et al.* The conclusions reached in the latter paper for a single model equation are consistent with that of Lettis (1987). If the imperfection is associated with end effects or wall undulations then it is appropriate to take $I_n(t)$ to be constant. We therefore set $I_n = 1$ until further notice. However we can show that the results found below are essentially independent of the time dependence of I_n, and for simplicity we shall confine our attention to the case when the imperfections are real. Thus when $\hat{R}_2 - \lambda^* G^2$ becomes positive some of the amplitudes grow rapidly to $O(1)$ values and remain $O(1)$ until local decay takes a disturbance amplitude down to a size fixed by that of the imperfection.

Suppose then that we allow the frequency Ω to tend to zero with $\gamma_n = O(\Omega)^{3/4}$. We shall here discuss the simplest case when $\gamma_n I_n$ is a constant and X_n are real and

write $\gamma_n I_n = \Omega^{3/4}\tilde{\gamma}_n$ where $\tilde{\gamma}_n$ is $O(1)$. If we define a new time scale $\bar{t} = \Omega t$ then (4.2) becomes

$$\Omega \frac{\mathrm{d}X_n}{\mathrm{d}\bar{t}} = \mu\{\hat{R}_2 - \lambda^* G^2\}X_n - \sum_{m=1}^{N} \omega_{mn} X_n |X_m|^2 + \tilde{\gamma}_n \Omega^{3/4}, \tag{4.3}$$

where G is given by (2.3a) with Ωt replaced by $\bar{t}$. The discussion of the previous Section shows that, with $\tilde{\gamma}_n = 0$, periodic finite-amplitude solutions of (4.3) bifurcate from the linear neutral points $\hat{R}_2 = R_2(\theta)$. On the other hand, for Ω sufficiently small, we expect that a finite-amplitude pure mode should exist whenever $\hat{R}_2 > \lambda^* G^2$. Indeed it is to be expected that, on the basis of quasi-steady theory, finite-amplitude mixed mode states with a different number of non-zero mode amplitudes will also be possible at different times during a period. In order to see how a switch from say M to $M-1$ modes takes place at some instant it is necessary to now take $\tilde{\gamma}_n \neq 0$. We therefore suppose that in some time interval $\bar{t}_1 < \bar{t} < \bar{t}_2$ a solution of (4.3) exists with, after ordering the modes in a suitable manner,

$$X_n = X_n(\bar{t}) + 0(\Omega)^{3/4}, \quad n = 1, 2, \ldots M,$$
$$X_n = \Omega^{3/4} X_n(\bar{t}) = \frac{\Omega^{3/4}\tilde{\gamma}_n}{\mu[\lambda^* G^2 - \hat{R}_2]} + \ldots, \quad n = M+1, \ldots N,$$

where the functions $X_n, n = 1, 2, \ldots, M$ are found by setting $\mathrm{d}/\mathrm{d}\bar{t} = 0, X_n = 0, n > M$, in (4.3), dividing through by X_n and solving the resulting M linear equations for X_n^2. The solution obtained in this way is valid so long as $X_n^2 > 0, n = 1, 2, \ldots M$. Whilst this is the case the M finite-amplitude modes evolve quite independently of the imperfection-driven modes $X_{M+1}, \ldots, X_N$. We note that the finite-amplitude modes are independent of the imperfection at leading order. Furthermore we also note that, at any given time, there will be several possible choices for M. Thus for example there will be a family of pure mode solutions with $M = 1$. These correspond to the single-mode solutions of (4.3) which exist wherever a mode is instantaneously unstable and its finite-amplitude state is stable to other linearly unstable perturbations. At any instant there will of course be a mode which is linearly the most unstable, i.e. the mode with $G = 0$, but that does not mean that it continues to dominate in the finite-amplitude state. In fact a secondary instability analysis of (4.3) with G held fixed shows that any pure mode eventually becomes stable against all perturbations so that, at any instant in time, no preferred mode can be identified by nonlinear theory. This means that at any instant the disturbance will depend on the nature of $\tilde{\gamma}_n$ and the previous history of the flow. More precisely it means that when the basic state evolves in time we should not necessarily expect that the disturbance pattern will be in the form of a roll pattern aligned in such a manner as to make $G = 0$.

Now let us see how the above expansions must be modified at a time when the number of $O(1)$ disturbances changes. Again we suppose that the modes have been conveniently ordered so that, when $\bar{t} = \bar{t}_2$, the Mth mode obtained from the solution procedure described above is found to have zero amplitude. The exponential decay of the Mth mode in the vicinity of $\bar{t}_2$ is halted by the imperfections in the system. This takes place in an $O(\Omega^{1/2})$ time interval near $\bar{t} = \bar{t}_2$; we therefore write

$$\hat{t} = \frac{[t - \bar{t}_2]}{\Omega^{1/2}}$$

and then, near $\bar{t}_2$, we write

$$X_n = X_n(\bar{t}_2) + O(\Omega^{1/2}), \quad n = 1, 2, \ldots M-1, \tag{4.4a}$$

$$X_M = \Omega^{1/4} X_M(\hat{t}) + O(\Omega^{1/2}), \tag{4.4b}$$

$$X_n = \frac{\Omega^{3/4}\tilde{\gamma}_n}{\mu[-\lambda^* G^2(\bar{t}_2) + \hat{R}_2] + \sum_{m=1}^{M-1} \omega_{mn}|X_m|^2}, \quad n = M+1, \ldots N. \tag{4.4c}$$

Here the quantities $X_n(\bar{t}_2), n = 1, M-1$, are obtained by solving

$$\mu(\hat{R}_2 - \lambda^* G^2(\bar{t}_2)) = \sum_{m=1}^{M-1} \omega_{mn}|X_m|^2, \quad n = 1, \ldots M-1,$$

whilst $X_m(\hat{t})$ satisfies the evolution equation

$$\frac{\mathrm{d}X_M}{\mathrm{d}\hat{t}} = \mu_M X_M \hat{t} - \alpha_M X_M^3 + \tilde{\gamma}_M, \tag{4.5}$$

where μ_M and α_M are negative and positive constants respectively.

The required solution of (4.5) has $X_M \sim |\hat{t}|^{1/2}$ when $\hat{t} \to -\infty$ and is such that $X_M \sim \tilde{\gamma}_M/\mu_M\hat{t}$ when $\hat{t} \to \infty$. This ensures a match between the solution in the transition layer and the local equilibrium state before and after this layer. Thus in an $O(\Omega^{1/2})$ interval a finite-amplitude mode decays into the background state. A similar analysis describes the growth out of the background of a single mode at some time $\bar{t} = \bar{t}_1$.

The above discussion shows that the periodic solutions of (4.2) with $\tilde{\gamma}_n = 0$ can be perturbed by $O(1)$ amounts when small imperfections are present. Thus, at any instant, for small frequencies any one of the instantaneously possible states can be excited by $O(\Omega^{3/4})$ imperfections. However, modes may amplify from, or decay into, the $O(\Omega^{3/4})$ background at any instant so that the convection pattern will vary over a period.

At sufficiently large values of $\hat{R}_2$ the periodic solutions of the imperfection-free problem are valid throughout a period and the amplitudes are perturbed only at $O(\Omega^{3/4})$. Thus imperfections only play a role when a local solution of the quasi-steady problem has one of its non-zero amplitudes vanishing at some instant.

It follows that the stabilizing effect found by Kelly & Hu (1993) for this flow is destroyed at frequencies of size $\hat{\gamma}^{4/3}$ where $\hat{\gamma}$ is the size any imperfections present in the system. Thus, if we think of $\hat{\gamma}$ as being fixed, when the frequency has been reduced to $O(\hat{\gamma}^{4/3})$, the system behaves in an effectively steady manner and at any instantaneously unstable time a variety of finite-amplitude states are possible. In fact we now show, using the ideas of Lettis (1987), that the linear selection mechanism of Kelly & Hu (1993) is destroyed at even larger values of the frequency. Clearly we need to identify the size of the frequency at which imperfections of size $O(\hat{\gamma})$ first have an $O(1)$ effect on the system. In the first instance we suppose that $\Omega \to 0$ with $\hat{\gamma} = O(\Omega^K), 0 < K$. For $0 < K \leqslant \frac{3}{4}$ the above analysis survives essentially intact whereas for $K > \frac{3}{4}$ the method of Lettis shows that the only significant change in structure occurs near the time $\bar{t} = \bar{t}_2$, where a mode either amplifies from or decays into the background state. Since the imperfection is now smaller a direct match through a single boundary layer at $\bar{t} = \bar{t}_2$ onto the algebraically growing or decaying

mode cannot be achieved. It turns out, see Lettis (1987), that the single boundary layer at $\bar{t} = \bar{t}_2$ must be replaced by two layers defined by

$$|\bar{t} - \bar{t}_2| \sim \left| \frac{\Omega}{|\ln \Omega|} \right|^{1/2}, \quad |\bar{t} - \bar{t}_2| \sim |\Omega \ln \Omega|^{1/2}.$$

Away from the outer layer, $|\bar{t} - \bar{t}_2| \sim O|\Omega \ln \Omega|^{1/2}$, imperfections play no significant role and at any instant a variety of possible states will again be possible. Thus, if $\hat{\gamma}$ is held fixed when the frequency has been reduced to $\hat{\gamma}^{1/K}$ for any $K > 0$, the linear selection mechanism of Kelly & Hu is not operational and the system behaves in a quasi-steady manner. Since the latter result is valid for all $K > 0$ it is to be expected that once Ω falls below an $O(1)$ value quasi-steady effects will dominate. In fact, as again was first shown by Lettis (1987), this is not quite true and there is a minimum, but small, size for Ω where this is the case. This limiting case can be seen either directly from (4.2) or by a more careful examination of the thickness of the outer boundary layer at $\bar{t} = \bar{t}_2$ for $\hat{\gamma} = O(\Omega^K)$ by taking the further limit $K \to \infty$. In the latter case we take K sufficiently large that the outer layer is of length $O(1)$. In this case the adjustment of a mode to or from a finite-amplitude state is now taking place on the time scale over which the non-vanishing modes evolve. The linear exponential growth then amplifies X_n to a size such that $\Omega \dot{X}_n \sim (\hat{R}_2 - \lambda^* G^2) X_n \sim \tilde{\gamma}_n$ near $\bar{t}_2$. Either of these approaches shows that the critical size of $\hat{\gamma}$ is given by

$$\hat{\gamma} = 0(\mathrm{e}^{-D/\Omega}) \tag{4.6}$$

for some constant D. In other words, if each disturbance is smaller than $O(\mathrm{e}^{-D/\Omega})$ for D sufficiently large, the linear exponential growth over the unstable parts of the period is not sufficient to stimulate any mode into its quasi-steady state. If we again think of $\hat{\gamma}$ being fixed it follows from (4.6) that when Ω is decreased from an $O(1)$ value the system is first able to respond in a quasi-steady manner when Ω falls to $O(|\ell \mathrm{n} \hat{\gamma}|^{-1})$. Hence even very small imperfections are important when the frequency is decreased from an $O(1)$ value. Now we shall report on some numerical solutions of (4.3) which illustrate the results of the above discussion.

The numerical integration of (4.3) was carried out using a fourth-order Runge–Kutta scheme. In the first instance we report on some solutions of (4.3) for an $O(1)$ value of the frequency. We take M in (4.3) to be 32 and define θ_n by

$$\theta_n = -\frac{\pi}{2} + \frac{(n-1)}{32}\pi, \quad n = 1, 2, ..., 32.$$

In the first case we choose $\gamma_n I_n = 10^{-3}$ for all n and the initial conditions were taken to be:

Case (a) $X_n = 0, \ n \neq 17, \quad X_{17} = 1$;,
Case (b) $X_n = 1, \ n = 1, 2, \ldots 32$;,
Case (c) $X_n = 0, \ n \neq 16, \ X_{16} = 1$.

The first case corresponds to an initial roll mode parallel to the y-axis. This is the most dangerous orientation for a disturbance on the basis of linear theory for the particular choice $\hat{\lambda}_1 = 1, \hat{\lambda}_2 = 2$. Figure 8 shows a few of the amplitudes X_n corresponding to the periodic solution obtained by integrating (4.3) with initial conditions (a) over a sufficient time interval and with $\lambda_1^* = R_2 = \sigma = 1$. We see that X_{17} is the only mode shown which has amplitude greater than that of the background state. In fact the modes not shown are also of small amplitude so that at all times

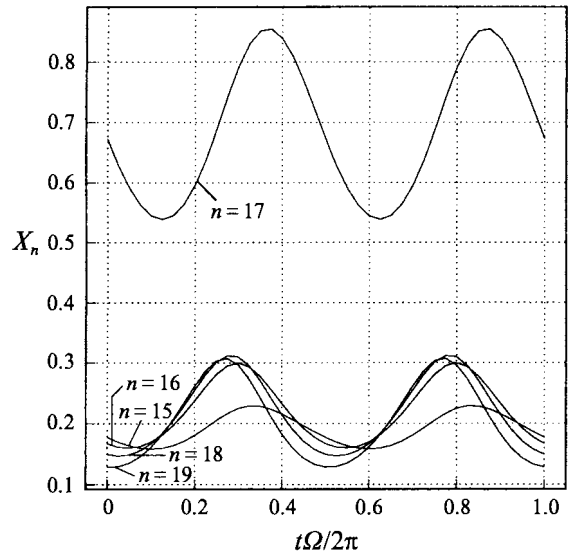

FIGURE 8. The periodic solution of (4.3) corresponding to initial conditions (*a*). In order to be seen on this scale the $n = 15, 16, 18, 19$ modes have been multiplied by 100.

the convection pattern is in the form of rolls aligned almost with the *y*axis. A similar calculation with (*c*) as initial conditions produced the same periodic solution. If the calculation is repeated with (*b*) as initial condition we obtain a picture similar to figure 8 except that the only mode greater than the background state is X_{16}=1. The results of these calculations therefore confirm the predictions of figure 2. Calculations with other initial conditions produced further periodic solutions with, in each case, a single $O(1)$ disturbance amplitude. However it could well be that a more exhaustive search might produce more complex periodic solutions with more than one amplitude being $O(1)$.

Next we discuss the solution of (4.3) with $\gamma_n \neq 0$. We shall again take $\lambda^* = \hat{R}_2 = \sigma = \hat{\lambda}_1 = 1, \hat{\lambda}_2 = 2, M = 32$. The initial conditions were taken to be $X_{17} = 1, X_n = 0, n \neq 17$ and we considered the following cases:

Case (*d*) $\gamma_n I_n = 10^{-11}$, $\Omega = 0.021$;
Case (*e*) $\gamma_n I_n = 10^{-1}$, $\Omega = 0.021$;
Case (*f*) $\gamma_n I_n = 0.01$, $\Omega = 1$.

The first two of the above cases correspond to a relatively small value of the frequency and the aim of the calculations was to confirm the results of our investigation into the role of imperfections in the low-frequency limit. In order to quantify the role of the imperfections in the pattern selection problem at low frequencies we have in figures 10, 11, 12 shown the perturbation temperature isotherms for the above cases at $z = \frac{1}{2}$ at the instants $\Omega t = 0, \pi/4, \pi/2, 3\pi/4, \pi, 5\pi/4, 3\pi/2, 7\pi/4$. Figure 9 describes a convection pattern with period π/Ω whereas the basic flow has period $2\pi/\Omega$. However solutions with period $2\pi/\Omega$ are also possible and one such flow is obtained by replacing γ_n by 10^{-5} in Case (*d*).

Figure 9 corresponds to imperfections of size 10^{-11} yet remarkably we see that the π/Ω-periodic solution shown is significantly altered from the pattern which would be found with $\gamma_n = 0$. In the absence of any imperfection the convection pattern would

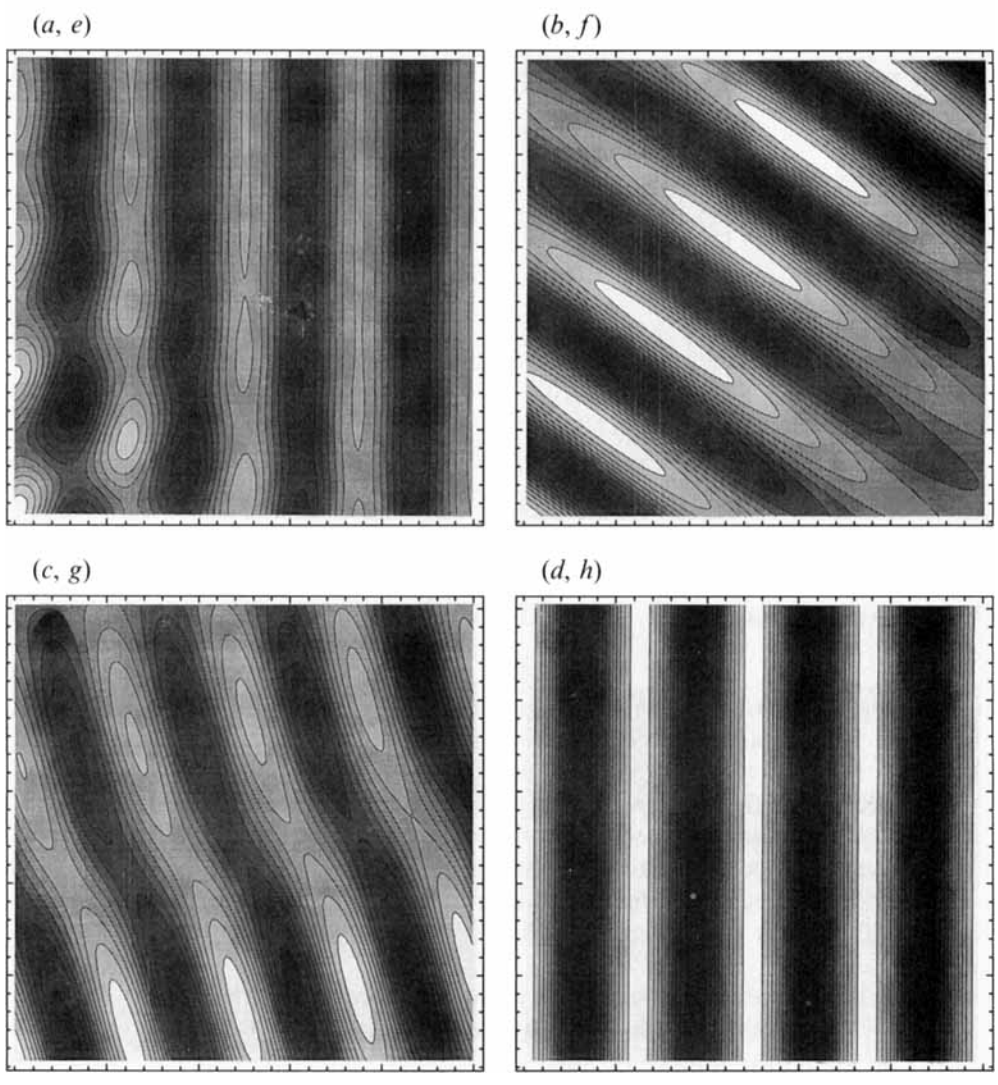

FIGURE 9(*a–h*). The contours of constant temperature perturbation at $\Omega t = 0, \pi/4, 3\pi/4, \pi, 5\pi/4, 3\pi/2, 7\pi/4$, with $z = \pi/2$ and conditions given by case (*d*). The horizontal and vertical axes correspond to x, y respectively and hot regions are represented by darker shading.

be in the form of rolls parallel to the y-axis. Figure 9 shows that the roll pattern is significantly perturbed away from the y-direction for most of the period. Further calculations showed that it was necessary to reduce γ_n to 10^{-15} before the rolls are, on the accuracy of figure 9, parallel to the y-axis throughout a period.

In figure 10 we see that at even higher imperfection amplitudes the pattern again has period π/Ω. In addition we now see that the oscillation deforms the straight roll pattern of the imperfection-free case into complicated curved cell patterns. The results we have obtained are therefore consistent with our analysis in that they show clearly the sensitivity of the system to imperfections at low frequencies. The fact that (4.3) has solutions which are either synchronous or subharmonic with the coefficients in that equation is not surprising. Some experimentation with initial conditions showed that the response is a function of initial conditions and the size of the imperfections.

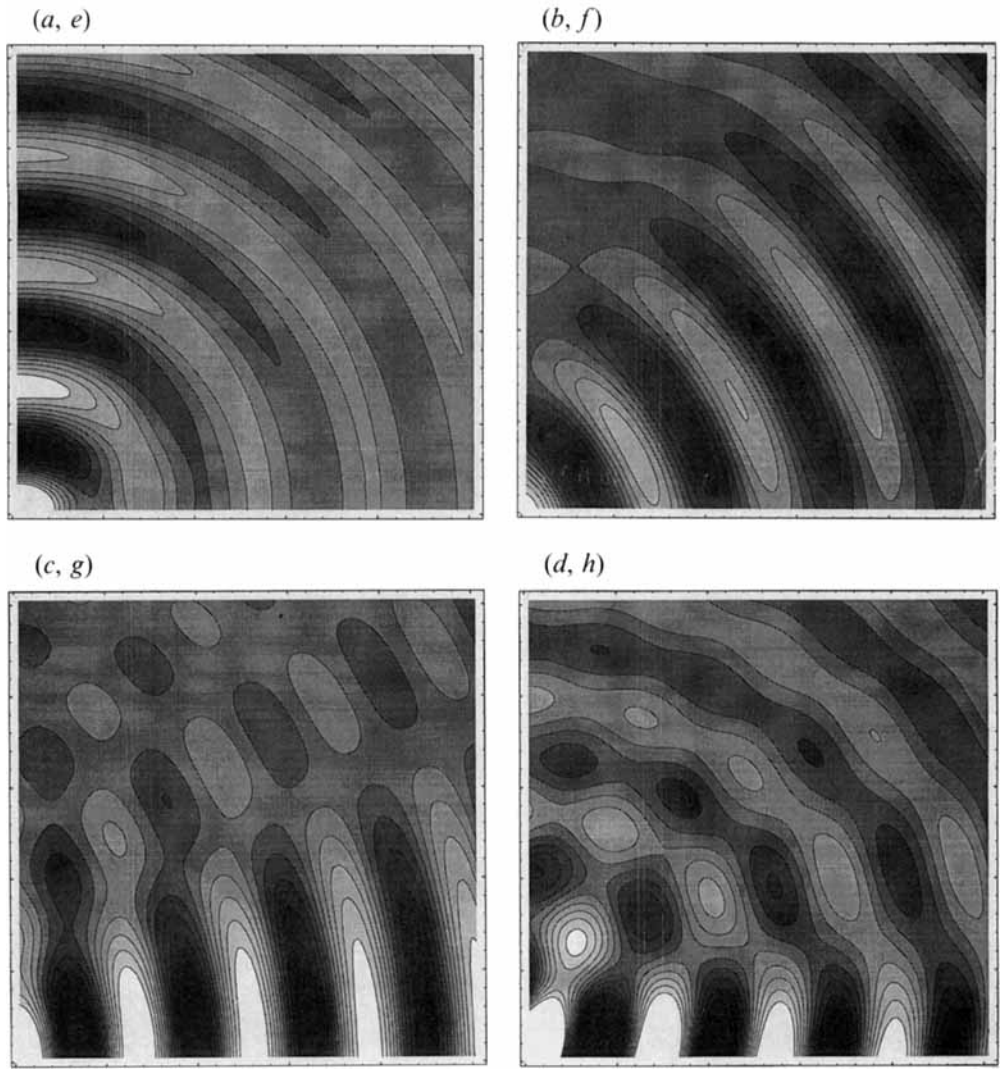

FIGURE 10 (*a–h*). The contours of constant temperature perturbation at $\Omega t = 0, \pi/4, 3\pi/4, \pi, 5\pi/4, 3\pi/2, 7\pi/4$, with $z = \pi/2$ and conditions given by case (*e*). The horizontal and vertical axes correspond to x, y respectively and hot regions are represented by darker shading.

In figure 11 we show the cell pattern corresponding to Case (*f*). At this much larger frequency we see that even a relatively large imperfection does not significantly alter the cell pattern from that predicted by an imperfection-free calculation.

Finally in figure 12 we show the results for the case when the imperfections are of a random nature. The results shown correspond to the same parameters as figure 10 with the exception that γ_n is now taken to be a random variable given by a normal distribution of mean 10^{-5} and variance unity. We now see once again that the randomly varying imperfection leads to a convection pattern which changes orientation through the period of oscillation of the basic flow.

It should be noted that all the results presented correspond to $M = 32$. Calculations at larger values of M produce similar results if the amplitudes are scaled appropriately.

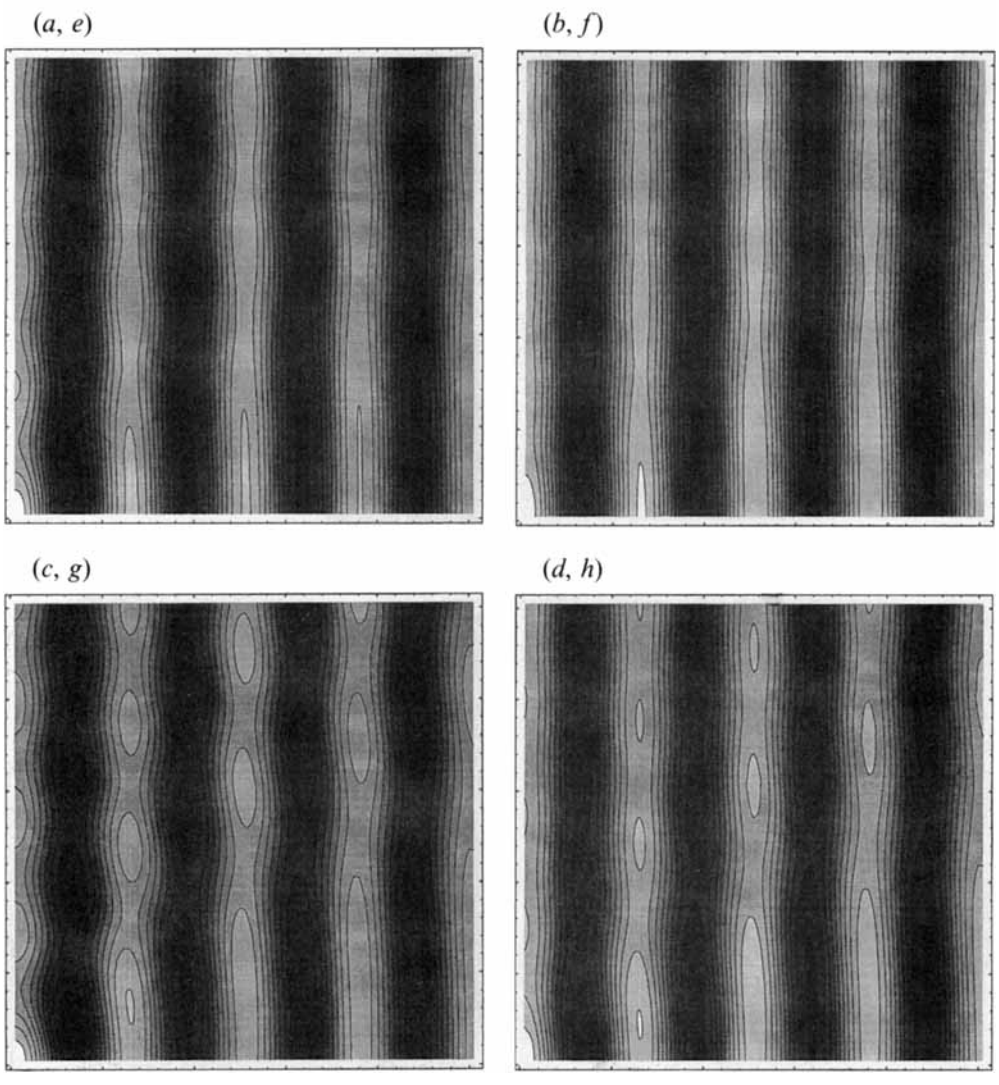

FIGURE 11 (*a–h*). The contours of constant temperature perturbation at $\Omega t = 0, \pi/4, 3\pi/4, \pi, 5\pi/4, 3\pi/2, 7\pi/4$, with $z = \pi/2$ and conditions given by case (*f*). The horizontal and vertical axes correspond to x, y respectively and hot regions are represented by darker shading.

More precisely it should be noted that the continuous case is approached by taking the limit $M \to \infty$ with $M\gamma_n$ held fixed.

5. Conclusions

We have investigated the effect of an unsteady shear flow on the planform of thermal convection. Previous linear work by Kelly & Hu (1993) had identified a selection mechanism for the roll orientation of a Boussinesq fluid in the presence of flow oscillations. In addition Kelly & Hu found that the effect of the oscillations was to stabilize the flow.

As a special case we investigated the limit of the Rayleigh number perturbation tending to zero. In that case the roll cells must line up close to the angle of the

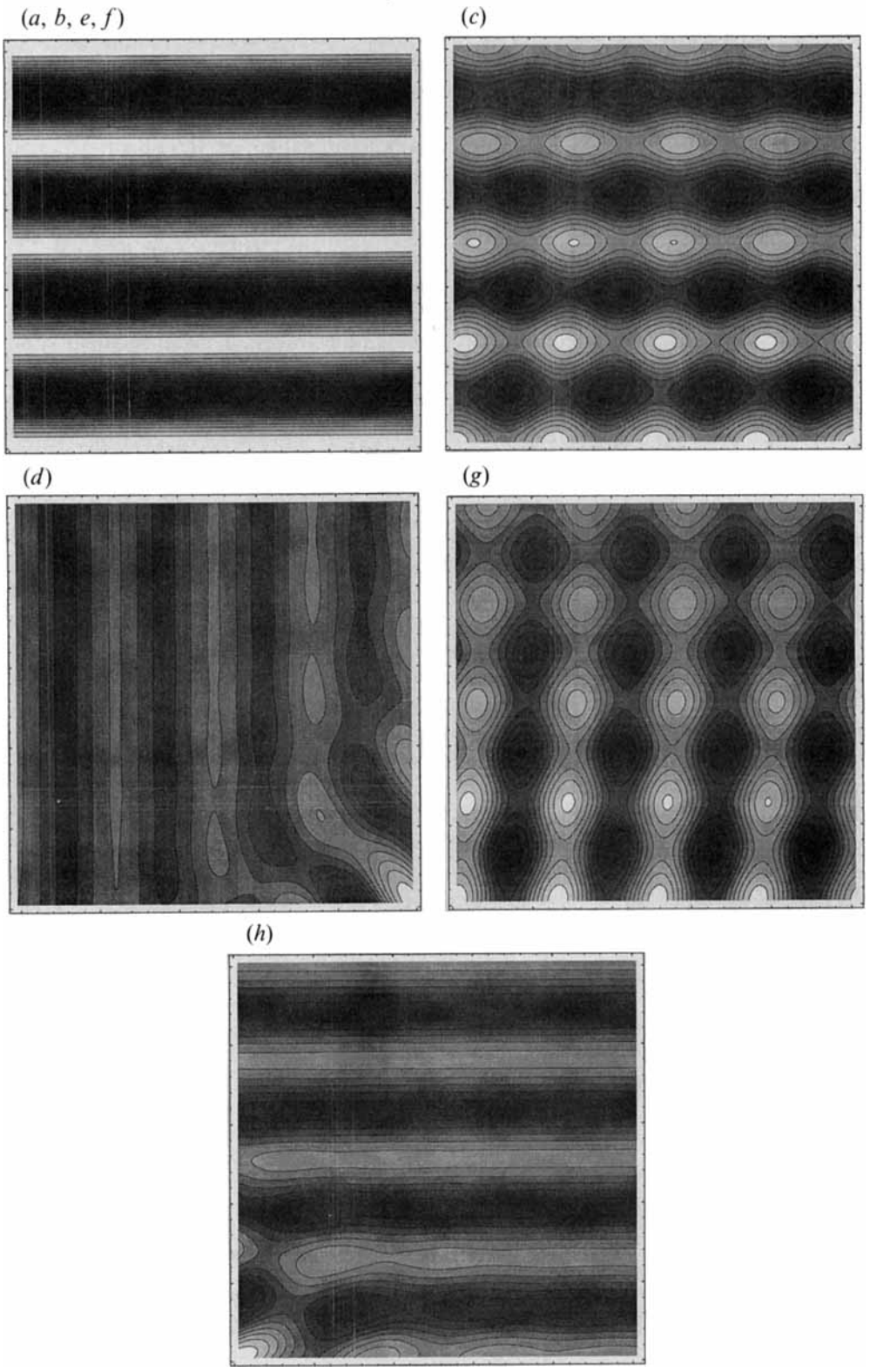

FIGURE 12 (*a–h*). The contours of constant temperature perturbation at $\Omega t = 0, \pi/4, 3\pi/4, \pi, 5\pi/4, 3\pi/2, 7\pi/4$, with $z = \pi/2$ and a randomly varying imperfection. The horizontal and vertical axes correspond to x, y respectively and hot regions are represented by darker shading.

most dangerous mode identified by the Kelly–Hu mechanism and the evolution of a packet of modes centred about that direction is determined as generalization of the Newell–Whitehead equation. However we found that there are significant differences from the zero shear case caused by the extra terms in the evolution equation. The most important difference is that, for certain fixed values of the shear, when the Rayleigh number is increased the roll pattern can become unstable and a jump to a new configuration will take place. Such a scenario is not possible for the Newell–Whitehead equation. Similarly if the Rayleigh number is held fixed and the shear flow amplitude decreased, so that the flow is linearly more unstable, the roll orientation must jump discontinuously because of the instability of certain roll orientations. Finally we note that the stabilizing mechanism found by Kelly & Hu persists into the nonlinear regime until imperfections play a role in the system. Thus, if in any practical application of the mechanism the size of the background noise can be determined, then, in order to achieve the full stabilizing effect of the oscillations, the time scale of the oscillations must be shorter than that over which the small imperfection has an effect on the convection amplitude.

In this paper we have investigated the nonlinear version of the problem considered by Kelly & Hu but concentrated on the low-frequency limit. We found that there is a critical size for the frequency below which imperfections present in the system play a crucial role and in effect cause the system to respond in a quasi-steady manner. In particular the stabilization found by Kelly & Hu is lost at sufficiently small frequencies so that, in the presence of small imperfections, the nonlinear problem is singular. By this we mean that, for a given small size of imperfection, the nonlinear solution at sufficiently small frequencies differs by an $O(1)$ amount from its value in the absence of imperfections. However another important result is that, even though at small enough frequencies the fluid responds in a quasi-steady manner, at any instant in time the convection cells do not line up in the direction associated with the direction identified as being the most unstable on the basis of linear theory. Thus, unlike what one might naively believe, the convection at small enough frequencies is not identical to that which would be seen for the corresponding steady case. Our calculations showed that in fact the cell pattern only resembles the expected straight roll for part of a period. At other times complicated curved cells are generated.

The author acknowledges some useful conversations with Professor R. E. Kelly in connection with the problem discussed here. The author also wishes to thank the referees and Professor R. E. Kelly for helpful comments on the original version of this paper. This research was supported by The National Science Foundation under Grant NSF CTS-9123553 and by the UK Science and Engineering Research Council.

REFERENCES

BARENGHI, C. F. & JONES, C. A. 1989 Modulated Taylor–Couette flow. *J. Fluid Mech.* **208**, 127.

BENOIT, E. 1990 *Dynamic Bifurcations, Proc. Luminy Conf.* Lecture Notes in Mathematics, vol. 149. Springer.

DIPRIMA, R. C. & STUART, J. T. 1975 The nonlinear calculation of Taylor vortex flows between eccentric rotating cylinders. *J. Fluid Mech.* **67**, 85.

HALL, P. 1975 The stability of unsteady cylinder flows. *J. Fluid Mech.* **67**, 29.

HALL, P. 1983 On the nonlinear instability of slowly varying time dependent flows. *J. Fluid Mech.* **126**, 357.

HALL, P. & KELLY, R. E. 1994 On the effect of a shear flow on the planform of thermal convection in a fluid of variable viscosity. Submitted for publication.

HALL, P. & WALTON, I. C. 1978 The smooth transition to a convective regime in a two-dimensional box. *Proc. R. Soc. Lond.* A **358**, 199.

KELLY, R. E. 1994 The onset and development of thermal convection in fully developed shear flows. *Adv. Appl. Mech.* **30**, 35.

KELLY, R. E. & HU, H.-C. 1993 The onset of Rayleigh–Bénard convection in non-planar oscillatory flows. *J. Fluid Mech.* **249**, 373.

KELLY, R. E. & HU, H.-C. 1994 The effect of finite amplitude non-planar flow oscillations upon the onset of Rayleigh-Bénard convection. *Heat Transfer 1994, Proc. 10th Intl Heat Transfer Conf.* (in press).

KELLY, R. E. & PAL, D. 1978 Thermal convection with spatially periodic boundary conditions: resonant wavelength excitation. *J. Fluid Mech.* **86**, 433.

LETTIS, D. S. L. 1987 The stability of time dependent flows. PhD thesis, Exeter University.

NEWELL, A. C. & WHITEHEAD, J. A. 1969 Finite bandwidth, finite amplitude convection. *J. Fluid Mech.* **38**, 279.

ROPPO, M. N., DAVIS, S. H. & ROSENBLAT, S. 1984 Bénard convection with time-periodic heating. *Phys. Fluids* **27**, 796.

SIGGIA, E. & ZIPPELIUS, E. 1981 Pattern selection in Rayleigh–Bénard convection near threshold. *Phys. Rev. Lett.* **47**, 835.